Could we see oscillations of the neutron star after the glitch in pulsar?

A.N. Timokhin

Sternberg Astronomical Institute, Moscow, Russia

Experimental study of NS structure

- Internal structure of celestial objects $\Longrightarrow$ need some kind of seismology

- In order to be able to proceed with seismological diagnostic two things are necessary:
  - Mechanism for oscillation excitation
  - Mechanism modulating radiation of the object

Observation of NS oscillations

- Neutron stars in binary systems:
  - Mechanism for oscillation excitation: instabilities in accretion flows.
  - Mechanism modulating radiation of the object: shaking of magnetic field lines, instabilities in boundary layer ...

  but, could we distinguish effects caused by oscillation of the *neutron star* and ones due to instabilities in the accretion flow? – which feature in the power spectrum corresponds to the *NS* oscillation and which to other processes?

- Isolated neutron stars – most of them radiopulsars:
  - Mechanism for oscillation excitation: **glitch**
  - Mechanism modulating radiation of the object: **this work**

Goldreich-Julian charge density and structure of the magnetosphere

Overview I

- We assume that NS is a conducting magnetized sphere on which surface an arbitrary velocity (vector) field is given. This field can be expanded in series of spheroidal and toroidal modes with harmonic numbers (l, m).
- We search for the special configuration of the electric field, such that, $\mathbf{E} \perp \mathbf{B}$ everywhere in the magnetosphere (force-free field). The charge density in the magnetosphere, supporting such electric field $\rho_{GJ} \equiv \nabla \cdot \mathbf{E}/(4\pi)$, is called Goldreich-Julian charge density.
- Assuming small physical current dencity in the magnetosphere, $j \ll \rho_{GJ}^{osc}\, c\ \ [c/(\nu_{osc} r)]$, we derive an equation for the electric potential of the force-free field in the near zone ($r \ll c/\nu_{osc}$) for any oscillation mode (l, m) and analyze its solutions.

Overview II

- To some extend we generalized the pulsar “standard model” to the case of arbitrary oscillations. This allows us to study the distortion of the magnetosphere caused by NS oscillations and estimate electromagnetic energy losses of an oscillating NS.
- This approximation is valid along open field lines for any oscillation mode and along closed field lines for oscillation modes with velocity field being symmetric relative to the equatorial plane.

Cosidered Cases

- Small amplitude oscillations of the NS with dipole magnetic field.
- Both **toroidal** ($\nabla \cdot V_{osc} = 0$) and **spheroidal** ($\nabla \times V_{osc} = 0$) oscillation modes were considered.
- Equation for Ψ_{GJ}can be solved analyticaly for both **toroidal** and **spheroidal** modes. Hence, Goldreich-Julian charge density can be calculated for any velocity field on the NS surface.
- **Examples**

  Spheroidal modes:

  Ψ_{GJ} (7,3); (7,2);

  ρ_{GJ} (7,3); (7,2);

  Toroidal modes:

  Ψ_{GJ} (1,0); (2,0); (2,1);

  ρ_{GJ} (1,0); (2,0); (2,1);

Distortion of the polar cap acceleration zone

Spheroidal Mode (44,4) and PSR J1824-2452

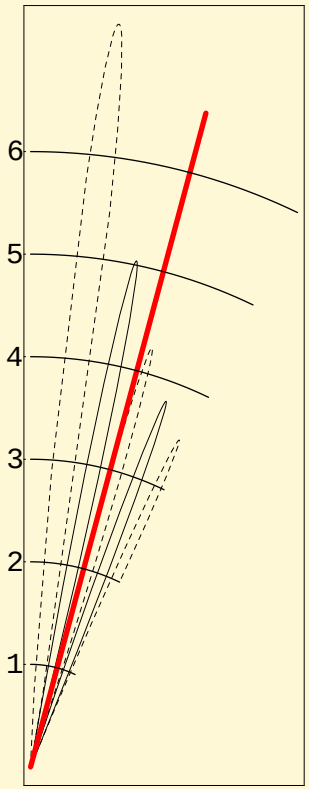

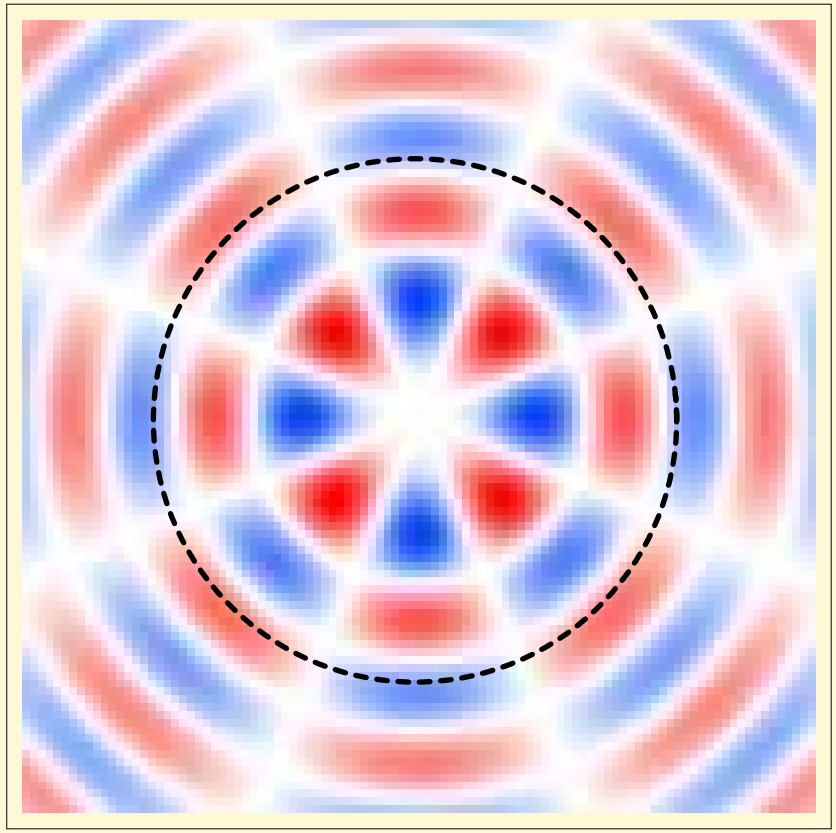

Figure 1: *left*: Goldreich-Julian Charge Density for oscillation mode $(44, 4)$ in polar coordinates $(\left|\rho_{GJ}^{lm}|_{r=r_*}\right|, \theta)$ for $\phi = 0$. The red line shows the angle at which the last closed fi eld line intersect the NS surface in PSR J1824-2452 (P=3.05 ms) *right*: The view of the PSR J1824-2452 polar cap (dashed circle). Goldreich-Julian Charge density for oscillation mode $(44, 4)$ is shown by the color map (red-positive, blue-negative)

GJ charge density: dependence on l

(24,4)

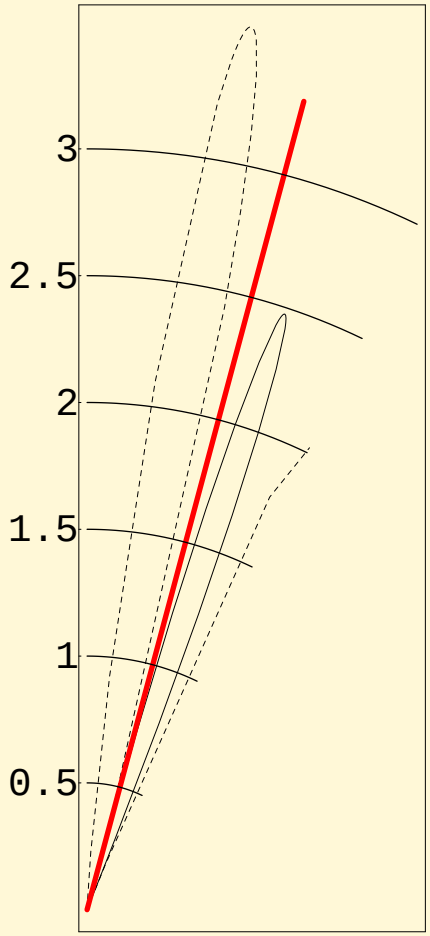

(44,4)

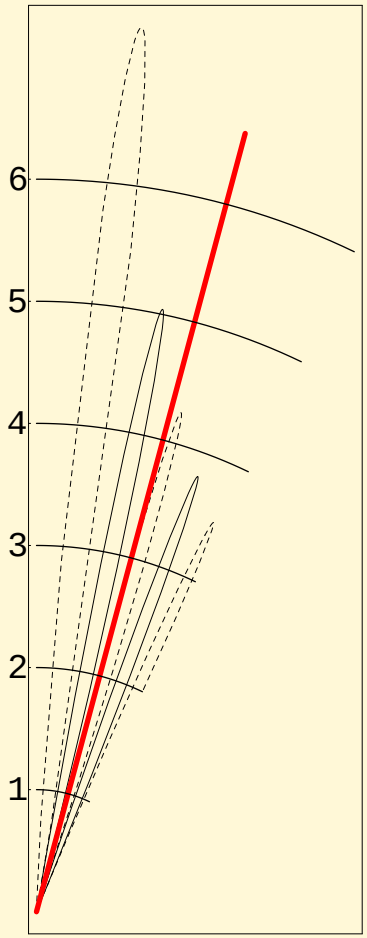

(64,4)

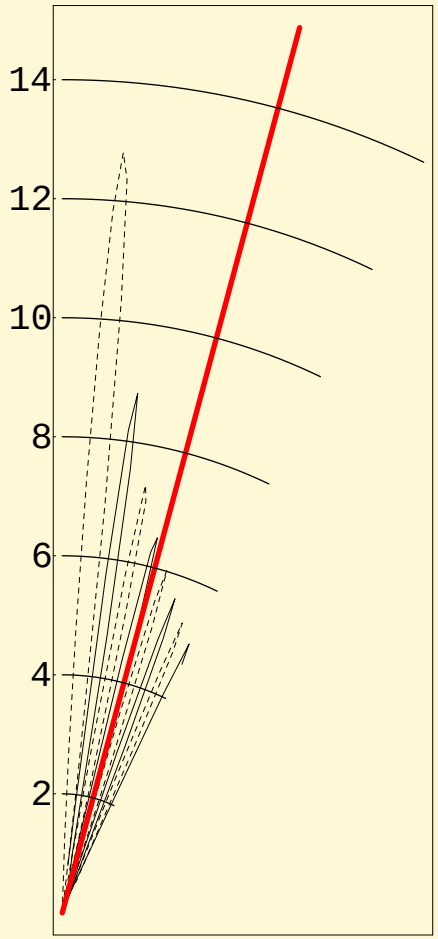

GJ charge density: dependence on m

(64,4)

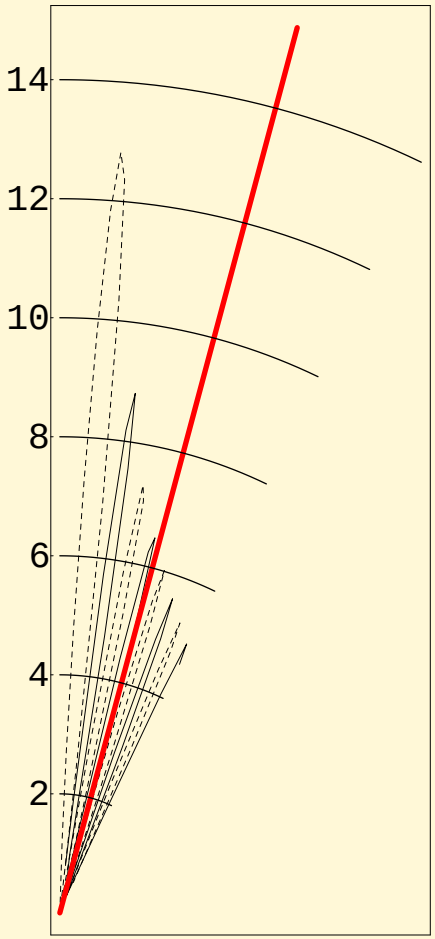

(64,8)

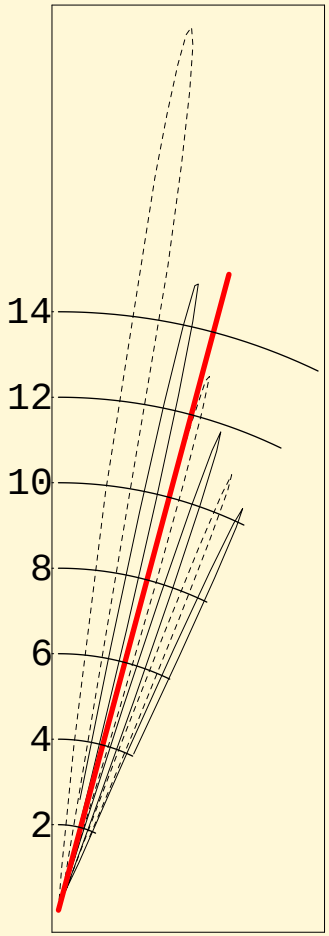

(64,14)

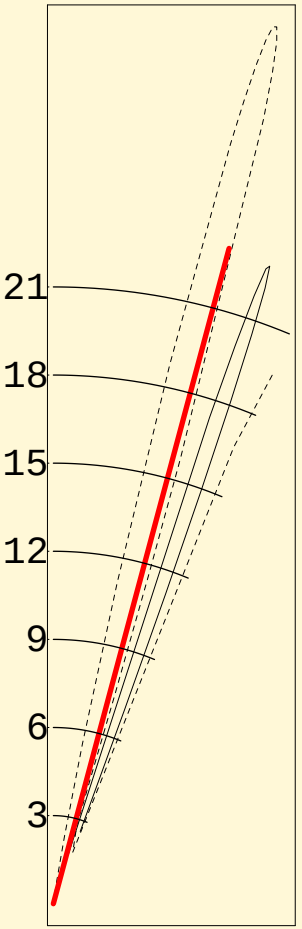

Oscillational GJ charge density

- The amplitude of ρ_{GJ} increases with increasing of the harmonic numbers l, m
  The reason:
  - the electric field

$$E \sim \frac{V_{osc}}{c} B$$

  - the charge density

$$\rho \sim \frac{E}{\delta x} \approx l \frac{E}{R}$$

- The amplitude of ρ_{GJ} for high harmonic numbers falls very rapidly with the distance from the NS

$E_{||}$ in the Polar Cap of pulsar for SCLF

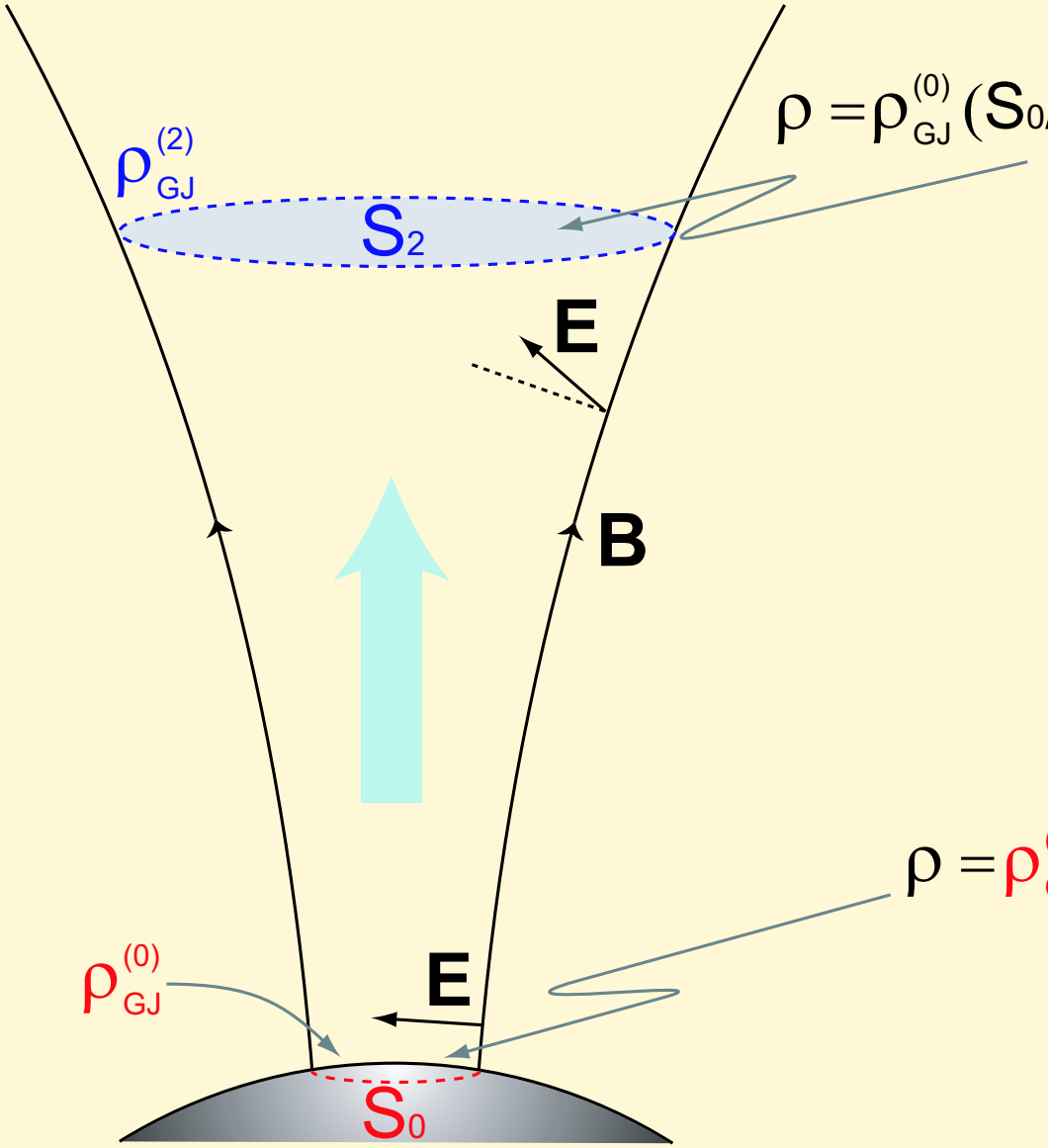

$$\rho = \rho_{GJ}^{(0)}(S_0/S_2) \neq \rho_{GJ}^{(2)},\ \mathbf{E}\cdot\mathbf{B}\neq 0$$

$$\rho = \rho_{GJ}^{(0)},\ \mathbf{E}\cdot\mathbf{B}=0$$

- If $\left|\rho_{GJ}^{(2)}\right| > |\rho|$ an accelerating electric fi eld is build up
- If $\left|\rho_{GJ}^{(2)}\right| < |\rho|$ there will be no particle acceleration at all ("decelerating fi eld")

Accelerating Potential: $\rho - \rho_{GJ}$ for $V_{rot} = V_{osc}$

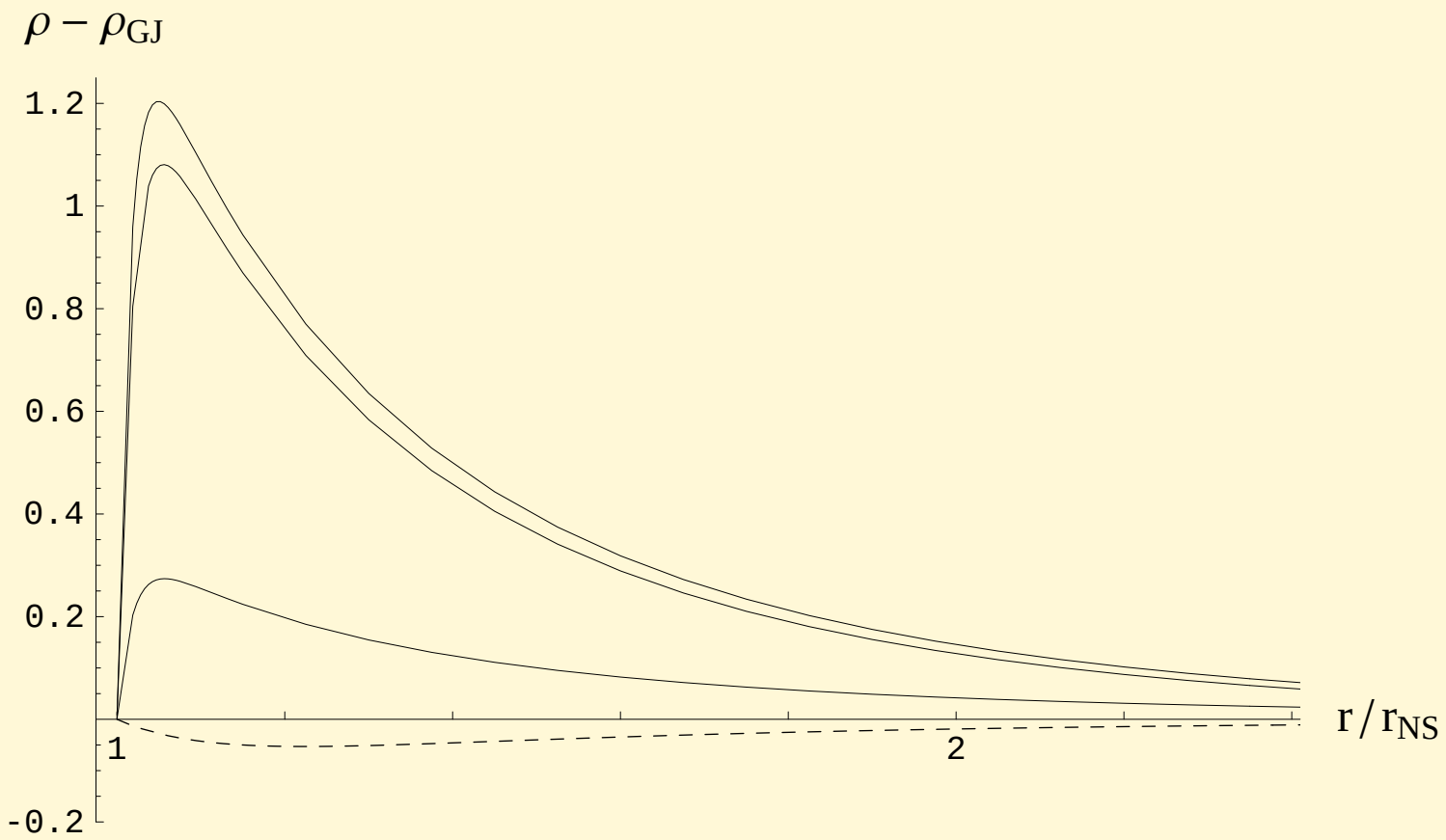

Figure 2: Difference between the charge density of space charge limited flow and the local Goldreich-Julian charge density along magnetic field lines in the polar cap region is shown (in arbitrary units) for three spheroidal modes with different (l, m): (64,14) – by the upper solid line, (54,14) – by the middle solid line, (54,2) – by the lower solid line. The same realtion for an aligned rotator is shown by the dashed line.

Velocity of oscillational motion

- Energy transferred during the glitch

$$W_{glitch} = I\Omega\Delta\Omega = I\Omega^2 \frac{\Delta\nu}{\nu} = i\, I_{NS} \left(\frac{2\pi}{P}\right)^2 \frac{\Delta\nu}{\nu}$$

- some fraction η of this energy goes to oscillation excitation

$$W_{osc} = \eta\, W_{glitch}$$

- Energy of oscillational motion

$$E_{osc} \simeq \frac{M_{osc} V_{osc}^2}{2} = \frac{\epsilon M_{NS} V_{osc}^2}{2}$$

- oscillational velocity

$$V_{osc} \simeq 500\, \eta_{\%}^{1/2}\, \epsilon^{-1/2}\, i^{1/2}\, P^{-1} \left(\frac{\Delta\nu}{\nu}\right)_6^{1/2} \mathrm{cm\ sec}^{-1}$$

Effective Goldreich-Julian charge density

- Electric fi eld induced by oscillations

$$E \simeq \frac{V_{osc}}{c} B$$

- Goldreich-Julian charge density for oscillational mode $(l, m) \sim \mathbf{l}$

$$\rho_{GJ}^{osc} \sim \frac{E}{\Delta x} \simeq \mathbf{l} \frac{E}{r_*} = \mathbf{l} \frac{V_{osc}}{c} \frac{B}{r_*}$$

- Efective Goldreich-Julian charge density
  - oscillational

$$\rho_{GJ}^{osc,eff} \sim \rho_{GJ}^{osc}$$

  - rotational – Muslimov & Tsygan model (particles freely escape NS surface)

$$\rho_{GJ}^{rot,eff} \sim \kappa \rho_{GJ}^{rot} \simeq .15 \ \rho_{GJ}^{rot}$$

  - rotational – Ruderman & Sutherland model (particles do not escape NS surface)

$$\rho_{GJ}^{rot,eff} \sim \rho_{GJ}^{rot}$$

Distortion of the accelerating electric field

Distortion of the accelerating electric fi eld in the polar cap is proportional to

$$\frac{\rho_{GJ}^{osc,eff}}{\rho_{GJ}^{rot,eff}}$$

- for Muslimov & Tsygan model

$$\frac{\rho_{GJ}^{osc,eff}}{\rho_{GJ}^{rot,eff}} \simeq 3.5 \times 10^{-3}\, l\, \eta_{\%}^{1/2}\, \epsilon^{-1/2}\, i^{1/2} \left(\frac{\Delta\nu}{\nu}\right)_6^{1/2}$$

- Ruderman & Sutherland model

$$\frac{\rho_{GJ}^{osc,eff}}{\rho_{GJ}^{rot,eff}} \simeq 5.3 \times 10^{-4}\, l\, \eta_{\%}^{1/2}\, \epsilon^{-1/2}\, i^{1/2} \left(\frac{\Delta\nu}{\nu}\right)_6^{1/2}$$

Harmonics where acceleration is damped

When $\frac{\rho_{GJ}^{osc,eff}}{\rho_{GJ}^{rot,eff}} \sim 1$ accleration of particles in the polar cap will be blocked periodically. This occurs

- for Muslimov & Tsygan model, when

$$l > 300\, \eta_{\%}^{-1/2}\, \epsilon^{1/2}\, i^{-1/2} \left(\frac{\Delta\nu}{\nu}\right)_6^{-1/2}$$

- Ruderman & Sutherland model, when

$$l > 2000\, \eta_{\%}^{-1/2}\, \epsilon^{1/2}\, i^{-1/2} \left(\frac{\Delta\nu}{\nu}\right)_6^{-1/2}$$

Possible observational signatures

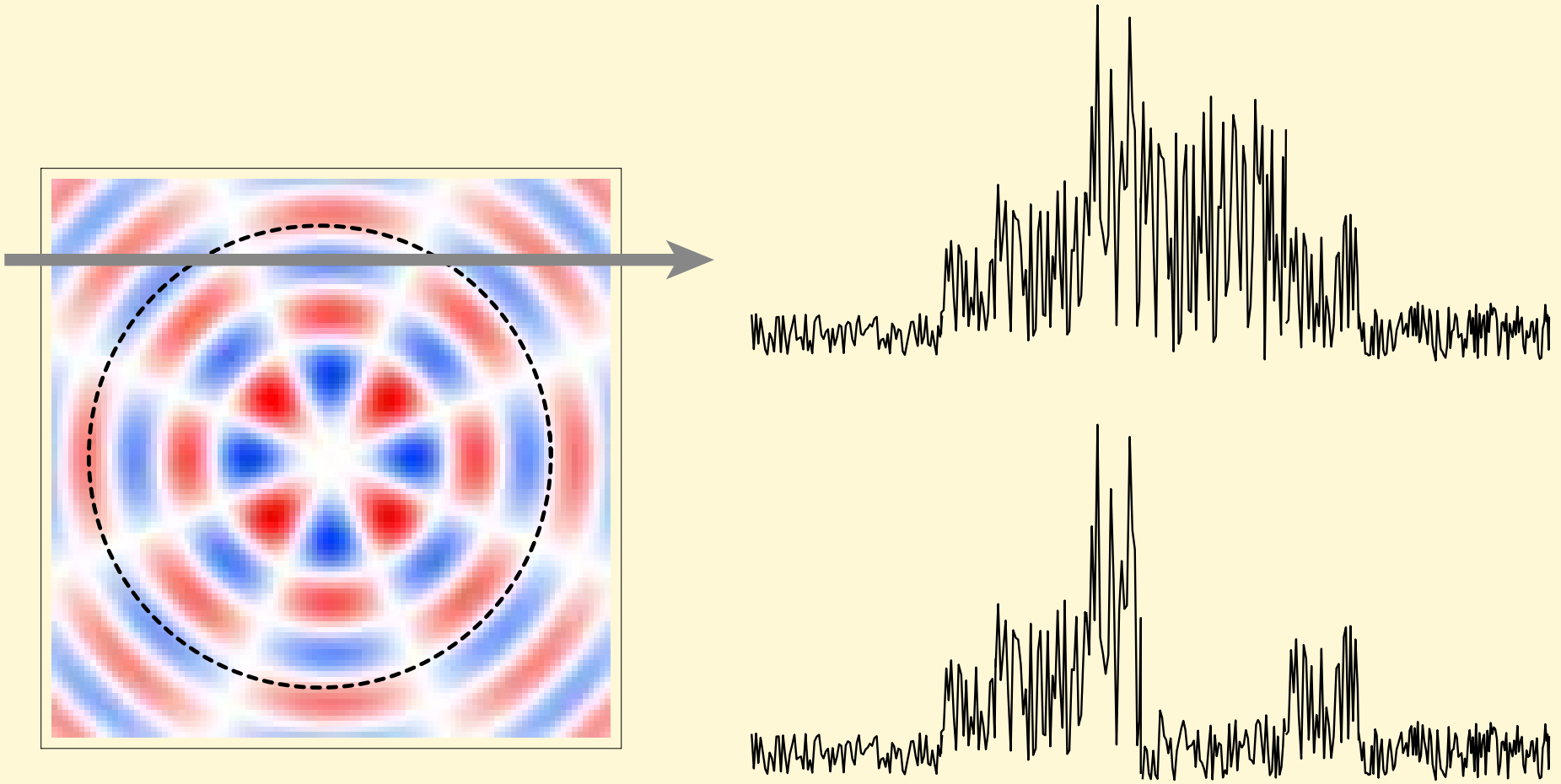

Figure 3: Schematic view of individual pulse distortion in pulsar due to oscillation of the netron star.

Conclusions

- In the polar cap region particle acceleration rate could be modulated with oscillation period. For oscillation modes with l, m large enough "decelerating" electric field could be of comparable strength with the accelerating field due to pulsar rotation even if $V_{\mathrm{osc}} << V_{\mathrm{rot}} = \Omega \mathrm{r}_*$
- For the half of oscillation modes a strong current ($\gg \rho_{\mathrm{GJ}} \mathrm{c}$) will flow along *closed* magnetic field lines

- Oscillations can distort acceleration of particles in the polar cap region of the pulsar and change its radiation pattern
- Distortion of the geometry of radiation region due to shaking of magnetic field lines is also possible, but is much more difficult to observe
- Region of closed field lines could become visible

Assumptions

- We consider the near zone $r \ll 2\pi\frac{c}{\omega}$ where

$$\frac{1}{c}\partial_t \mathbf{E} \ll \nabla\times\mathbf{B}$$

- We assume that the physical current density in the magnetosphere is low enough – the magnetic field to first order in $\tilde{\xi} \equiv \xi/r_*$ can be considered as generated only by volume currents inside the NS and by surface currents on its surface, i.e.

$$\frac{4\pi}{c}\mathbf{j} \ll \nabla\times\mathbf{B}^{(1)} \sim \frac{l}{r}\left(B^{(0)}\frac{\xi}{r_*}\right)$$

- The latter implies

$$j \ll \frac{B\xi\omega l}{4\pi c r_*}\, c\, \frac{c}{r\omega} \simeq \rho_{GJ}(r_*)\, c\, \left(\frac{c}{\omega r}\right)$$

Basic Equations

- **Maxwell Equations**

$$\nabla \cdot \mathbf{E} = 4\pi\rho \quad (1)$$

$$\nabla \times \mathbf{E} = -\frac{1}{c}\partial_t \mathbf{B} \quad (2)$$

$$\nabla \cdot \mathbf{B} = 0 \quad (3)$$

$$\nabla \times \mathbf{B} = 0 \quad (4)$$

- **Boundary Conditions**

$$B_r(r_*) = B_{0r}$$

$$E_{\theta,\phi}(r_*) = -\frac{1}{c}(\mathbf{v}\times\mathbf{B}_0)_{\theta,\phi}$$

Equation for E_{GJ}

- **General Solution of the Maxwell equations**
  From (3), (4) it follows [Muslimov & Tsygan 1986]:

$$\mathbf{B} = \nabla \times \nabla \times (P\mathbf{e}_r)$$

  Substituting $\mathbf{B}$ into equation (2) we get

$$\mathbf{E} = -\frac{1}{c}\nabla \times (\partial_t P\mathbf{e}_r) - \nabla\Psi \qquad (5)$$

- **Equation for the electric field**
  We are looking for a charge density ρ_{GJ} yielding $\mathbf{E} \perp \mathbf{B}$

$$\mathbf{E}_{GJ} \cdot \mathbf{B} = 0 \qquad (6)$$

$$\rho_{GJ} = \frac{1}{4\pi}\nabla \cdot \mathbf{E}_{GJ} = -\frac{1}{4\pi}\Delta\Psi_{GJ} \qquad (7)$$

  substituting $\mathbf{E}$ from the expression for the general solution of Maxwell Equations (5) into equation (6) we get

Equation for the Goldreich-Julian potential Ψ_{GJ}

$$\Delta_\Omega P\, \partial_r \Psi_{GJ} - \partial_r \partial_\theta P\, \partial_\theta \Psi_{GJ} - \frac{1}{\sin^2\theta}\, \partial_r \partial_\phi P\, \partial_\phi \Psi_{GJ} + \\ + \frac{1}{c \sin\theta} \{\partial_r \partial_\phi P\, \partial_\theta \partial_t P - \partial_r \partial_\theta P\, \partial_\phi \partial_t P\} = 0 \qquad (8)$$

+ **boundary conditions**

Equation for the Goldreich-Julian potential Ψ_{GJ}

$$\Delta_\Omega P\ \partial_r \Psi_{GJ} - \partial_r\partial_\theta P\ \partial_\theta \Psi_{GJ} - \frac{1}{\sin^2\theta}\ \partial_r\partial_\phi P\ \partial_\phi \Psi_{GJ} + \\ + \frac{1}{c\sin\theta}\left\{\partial_r\partial_\phi P\ \partial_\theta\partial_t P - \partial_r\partial_\theta P\ \partial_\phi\partial_t P\right\} = 0 \qquad (8)$$

+ boundary conditions

- The terms in gray boxes are coefficients depending on the unperturbed magnetic field configuration, they do not depend on the concrete oscillation mode.

Equation for the Goldreich-Julian potential Ψ_{GJ}

$$\Delta_\Omega P\ \partial_r \Psi_{GJ} - \partial_r\partial_\theta P\ \partial_\theta \Psi_{GJ} - \frac{1}{\sin^2\theta}\ \partial_r\partial_\phi P\ \partial_\phi \Psi_{GJ} + \\ + \frac{1}{c\sin\theta}\left\{\partial_r\partial_\phi P\ \partial_\theta\partial_t P - \partial_r\partial_\theta P\ \partial_\phi\partial_t P\right\} = 0 \qquad (8)$$

+ boundary conditions

- The terms in gray boxes are coefficients depending on the unperturbed magnetic field configuration, they do not depend on the concrete oscillation mode.
- Terms with $\partial_t P$ describe perturbations of the magnetic field by the stellar oscillations and are different for each oscillation mode (l, m).

Equation for the Goldreich-Julian potential Ψ_{GJ}

$$\Delta_\Omega P\ \partial_r \Psi_{GJ} - \partial_r\partial_\theta P\ \partial_\theta \Psi_{GJ} - \frac{1}{\sin^2\theta}\ \partial_r\partial_\phi P\ \partial_\phi \Psi_{GJ} + \\ + \frac{1}{c\sin\theta}\left\{\partial_r\partial_\phi P\ \partial_\theta\partial_t P - \partial_r\partial_\theta P\ \partial_\phi\partial_t P\right\} = 0 \qquad (8)$$

+ boundary conditions

- The terms in gray boxes are coefficients depending on the unperturbed magnetic field configuration, they do not depend on the concrete oscillation mode.
- Terms with $\partial_t P$ describe perturbations of the magnetic field by the stellar oscillations and are different for each oscillation mode (l, m).

This equation is linear PDE of the first order. Hence, oscillation modes can be considered separtely.

Rotation around z axis – Pulsar

- In this case the partial derivative ∂_t can be replaced by $-\Omega\,\partial_\phi$, where Ω is the angular velocity. Thus

$$\partial_t P = -\Omega\,\partial_\phi P$$

By direct substitution of

$$\Psi_{GJ} = -\frac{\Omega}{c}\sin\theta\,\partial_\theta P \tag{9}$$

it can be shown that the potential (9) is a solution of the equation (8) from the previous slide, and satisfies the boundary conditions for Ψ_{GJ}.

- For electric field and charge density we get

$$\begin{aligned}\mathbf{E}_{GJ} &= -\frac{1}{c}(\Omega\times\mathbf{r})\times\mathbf{B}\\ \rho_{GJ} &= -\frac{\Omega\cdot\mathbf{B}}{2\pi c}+\frac{1}{4\pi c}(\Omega\times\mathbf{r})\cdot(\nabla\times\mathbf{B})\end{aligned}$$

Goldreich & Julian (1969), Mestel (1971)

Boundary Conditions

- **Magnetic field**

$$\mathbf{B} = \nabla\times\nabla\times P\mathbf{e}_r\,, \quad \text{to the first order in } \frac{\xi}{r} : P \approx P_0(r,\theta,\phi) + \delta P(t,r,\theta,\phi)$$

$$\partial_t\,\delta P = \sum_{l,m}\left(\frac{r_*}{r}\right)^l \partial_t\,\delta p_{lm}(t)\,Y_{lm}(\theta,\phi)$$

$$\partial_t\,\delta p_{lm}(t) = \frac{1}{l(l+1)}\int_{4\pi} d\Omega\, Y^*_{lm}\,\{\mathbf{v}\cdot\nabla(\Delta_\Omega P_0)+ \\ +\Delta_\Omega P_0\,(\nabla\cdot\mathbf{v}_\perp) + r^2(\nabla_\perp(\partial_r P_0)\cdot\nabla_\perp)\,v_r\Big\}\Big|_{r=r_*}$$

- **Boundary Conditions for Ψ_{GJ}**

$$\Psi_{GJ}|_{r=r_*} = -\frac{1}{c}\int\left\{\frac{1}{r}\Delta_\Omega P_0\,v_\phi + \frac{1}{\sin\theta}\partial_r\partial_\phi P_0\,v_r + \frac{1}{\sin\theta}\partial_\phi\partial_t\delta P\right\} d\theta\Big|_{r=r_*} + e^{-i\omega t}F(\phi)$$

$$\Psi_{GJ}|_{\theta=0;\,r=r_*} = 0$$

Oscillation modes

- The oscillation velocity components for spheroidal ($\nabla \times \boldsymbol{\nu} = 0$) oscillations are

$$\nu_r = e^{-i\omega t}\, U(r)\, Y_{lm}(\theta,\phi), \quad \nu_\theta = e^{-i\omega t}\, V(r)\, \partial_\theta Y_{lm}(\theta,\phi),$$
$$\nu_\phi = e^{-i\omega t}\, V(r)\, \frac{1}{\sin\theta}\partial_\phi Y_{lm}(\theta,\phi)$$

  where U and V are radial and transversal velocity amplitude respectively.

- The oscillation velocity components for toroidal ($\nabla \cdot \boldsymbol{\nu} = 0$) oscillations are

$$\nu_r = 0, \quad \nu_\theta = e^{-i\omega t}\, W(r)\, \frac{1}{\sin\theta}\partial_\phi Y_{lm}(\theta,\phi), \quad \nu_\phi = -e^{-i\omega t}\, W(r)\, \partial_\theta Y_{lm}(\theta,\phi)$$

  where W is transversal velocity amplitude.

Toroidal Oscillations

- Equation for Ψ_{GJ}

$$2\cos\theta\,\partial_r\Psi^{lm}_{GJ}+\frac{1}{r}\sin\theta\,\partial_\theta\Psi^{lm}_{GJ}-\frac{m^2}{l(l+1)}\frac{B_0 w}{c}\left(\frac{r_*}{r}\right)^{l+1}Y_{lm}=0$$

- Boundary conditions

$$\begin{aligned}\Psi^{lm}_{GJ}|_{r=r_*} &= -\frac{B_0 w r_*}{c}\int\left(\cos\theta\,\partial_\theta Y_{lm}-\frac{m^2}{l(l+1)}\frac{Y_{lm}}{\sin\theta}\right)d\theta+e^{-i\omega t}\,F(\phi)\,,\\ \Psi^{lm}_{GJ}|_{\theta=0,r=r_*} &= 0\,.\end{aligned}$$

- Solution

$$\Psi^{lm}_{GJ}=\frac{m^2}{l(l+1)}\frac{B_0 W r_*}{c}\left(\frac{r_*}{r}\right)^{l}\sin^{2l}\theta\int\frac{Y_{lm}}{(\sin\theta)^{2l+1}}\,d\theta+\Phi_{lm}\left(\sin\theta\left(\frac{r_*}{r}\right)^{1/2},\phi,t\right)$$

Spheroidal oscillations

- Equation for Ψ_{GJ}

$$2\cos\theta\,\partial_r\Psi^{lm}_{GJ}+\frac{1}{r}\sin\theta\,\partial_\theta\Psi^{lm}_{GJ}-\frac{B_0}{c}\left[Z_1\left(\frac{r_*}{r}\right)^l\partial_\phi Y^m_{l-1}+Z_2\left(\frac{r_*}{r}\right)^{l+2}\partial_\phi Y^m_{l+1}\right]=0\,,$$

where

$$Z_1=\frac{1}{l}((l+1)V-U/2)\sqrt{\frac{l^2-m^2}{4l^2-1}}\qquad Z_2=\frac{1}{l+1}(lV+U/2)\sqrt{\frac{(l+1)^2-m^2}{(2l+3)(2l+1)}}$$

- Boundary conditions

$$\Psi^{lm}_{GJ}|_{r=r_*}=-\frac{B_0\,r_*}{c}\int\left(V\cot\theta\,\partial_\phi Y_{lm}-Z_1\frac{\partial_\phi Y^m_{l-1}}{\sin\theta}-Z_2\frac{\partial_\phi Y^m_{l+1}}{\sin\theta}-\right)d\theta+e^{-i\omega t}\,F(\phi)\,,$$

$$\Psi^{lm}_{GJ}|_{\theta=0,r=r_*}=0$$

- Solution

$$\Psi^{lm}_{GJ}=-\frac{B_0\,r_*}{c}\left\{Z_1\left(\frac{r_*}{r}\right)^{l-1}(\sin\theta)^{2l-2}\int\frac{\partial_\phi Y^m_{l-1}}{(\sin\theta)^{2l-1}}\,d\theta+\right.$$
$$\left.Z_2\left(\frac{r_*}{r}\right)^{l+1}(\sin\theta)^{2l+2}\int\frac{\partial_\phi Y^m_{l+1}}{(\sin\theta)^{2l+3}}\,d\theta\right\}+\Phi_{lm}\left(\sin\theta\left(\frac{r_*}{r}\right)^{1/2},\phi,t\right)$$

Spheroidal mode (7,3)

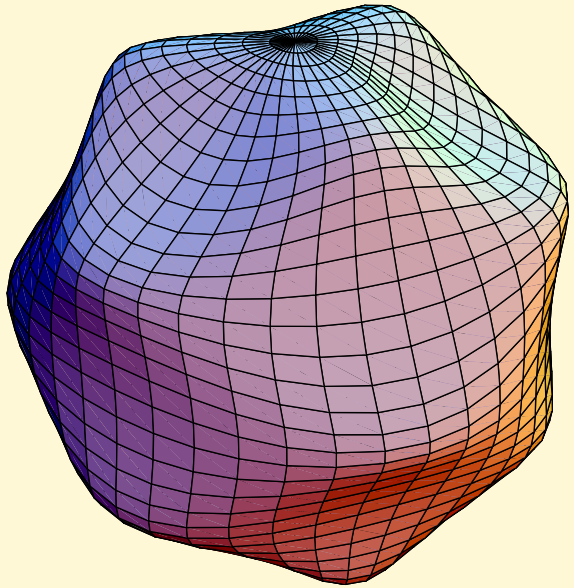

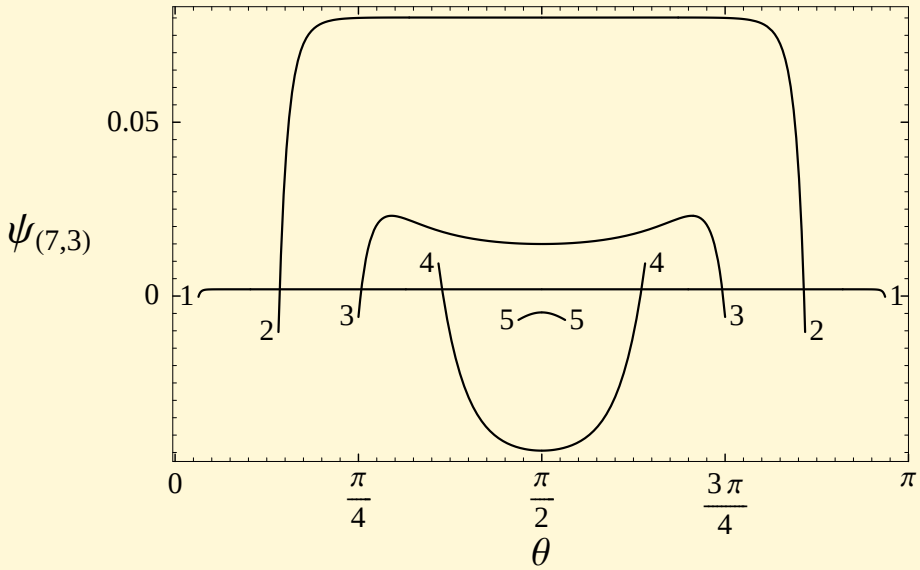

Figure 4: *left*: Deformation of the star surface during oscillation in spheroidal mode $(7,3)$ *right*: The potential Ψ_{GJ}^{73} along a dipolar magnetic fi eld line as a function of the polar angle θ is shown for 5 fi eld lines with azimuthal angle $\phi = 0$ at $t = 2\pi n/\omega$.

Spheroidal mode (7,3): GJ charge density

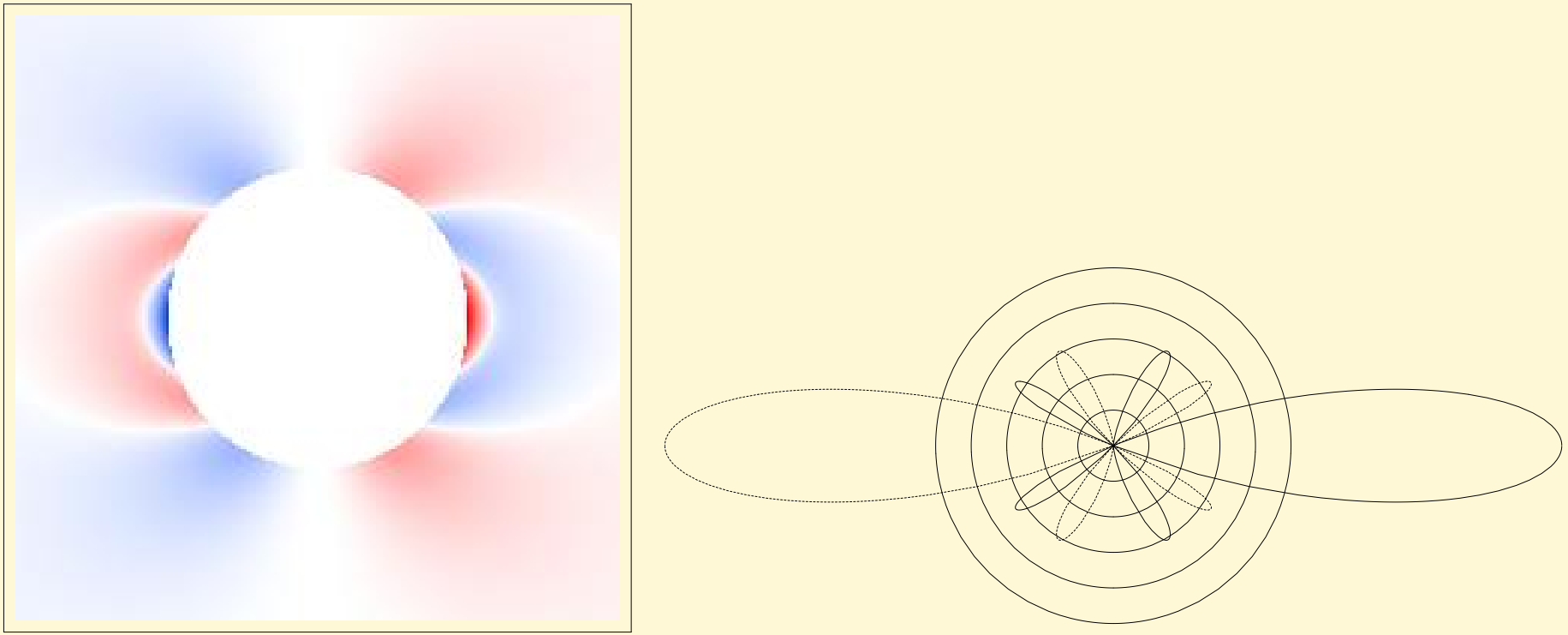

Figure 5: *left*: The charge density ρ_{GJ}^{73} near the NS for azimuthal angle $\phi = 0$ at $t = 2\pi n/\omega$. Positive values of charge density are shown by red and negative ones by blue color. *right*: The charge density $\rho_{GJ}^{73}|_{r=r_*}$ on the NS surface is shown in a polar coordinate system $(\left|\rho_{GJ}^{lm}|_{r=r_*}\right|, \theta)$ for $\phi = 0$. Positive values of charge density are shown by the solid line and negative ones by the dashed line.

Spheroidal mode (7,2)

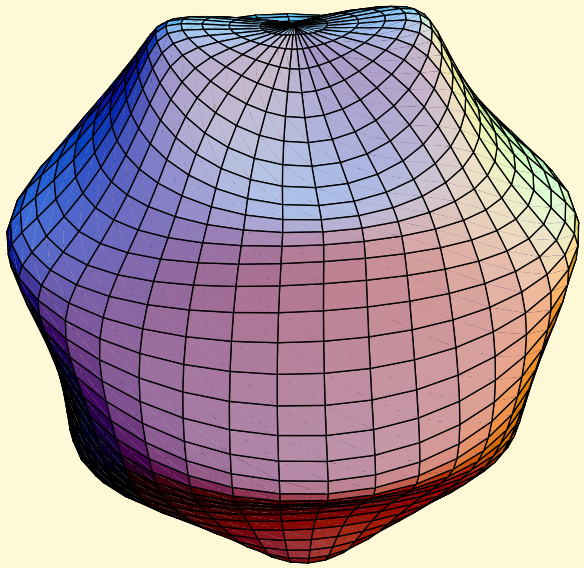

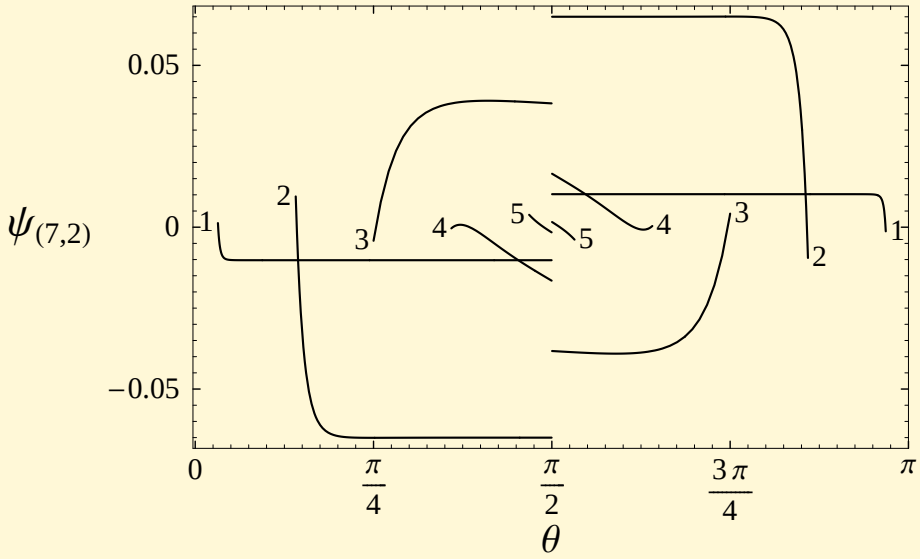

Figure 6: *left*: Deformation of the star surface during oscillation in spheroidal mode $(7,2)$ *right*: The potential $\Psi_{\rm GJ}^{72}$ along a dipolar magnetic fi eld line as a function of the polar angle θ is shown for 5 fi eld lines with azimuthal angle $\phi = 0$ at $t = 2\pi n/\omega$.

Spheroidal mode (7,2): GJ charge density

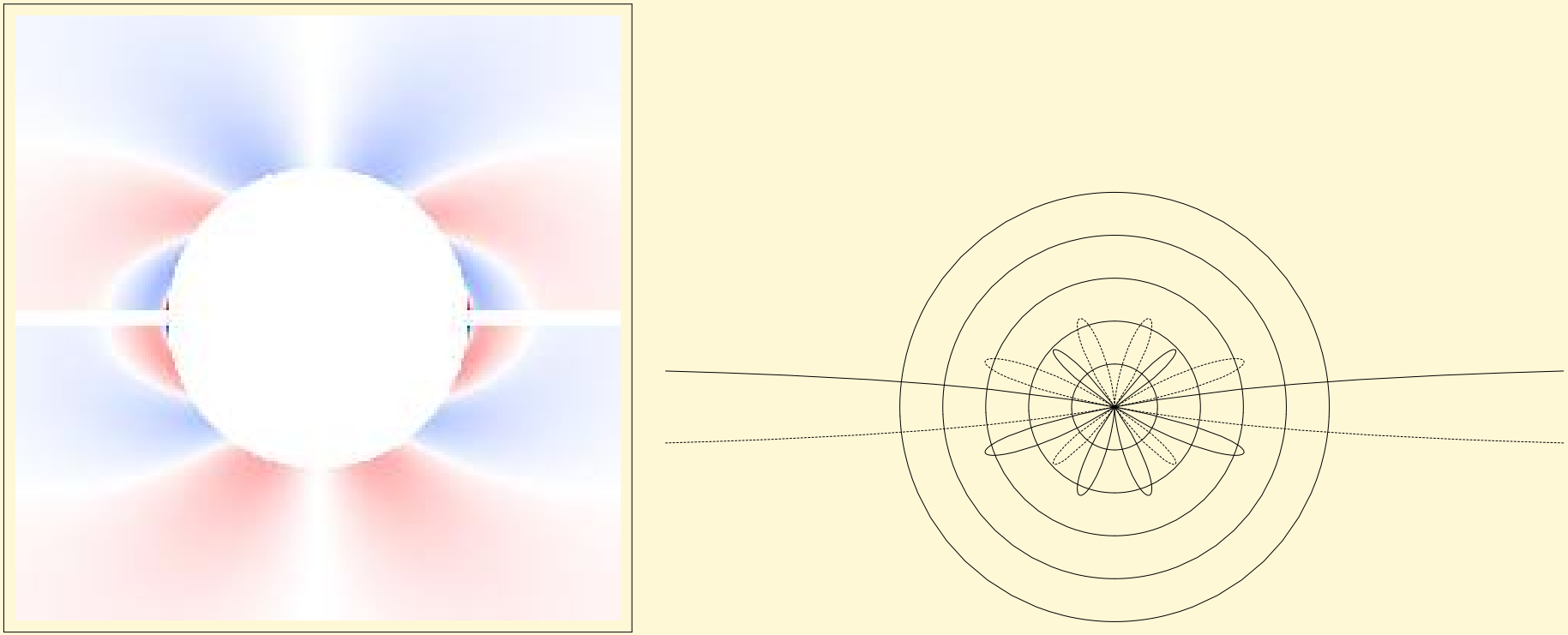

Figure 7: *left*: The charge density ρ_{GJ}^{72} near the NS for azimuthal angle $\phi = 0$ at $t = 2\pi n/\omega$. Positive values of charge density are shown by red and negative ones by blue color. *right*: The charge density $\rho_{GJ}^{72}|_{r=r_*}$ on the NS surface is shown in a polar coordinate system $(|\rho_{GJ}^{lm}|_{r=r_*}|, \theta)$ for $\phi = 0$. Positive values of charge density are shown by the solid line and negative ones by the dashed line. NB: on the equatorial plane ($\theta = \pi/2$) ρ_{GJ}^{72} is infinite.

Toroidal mode (1,0)

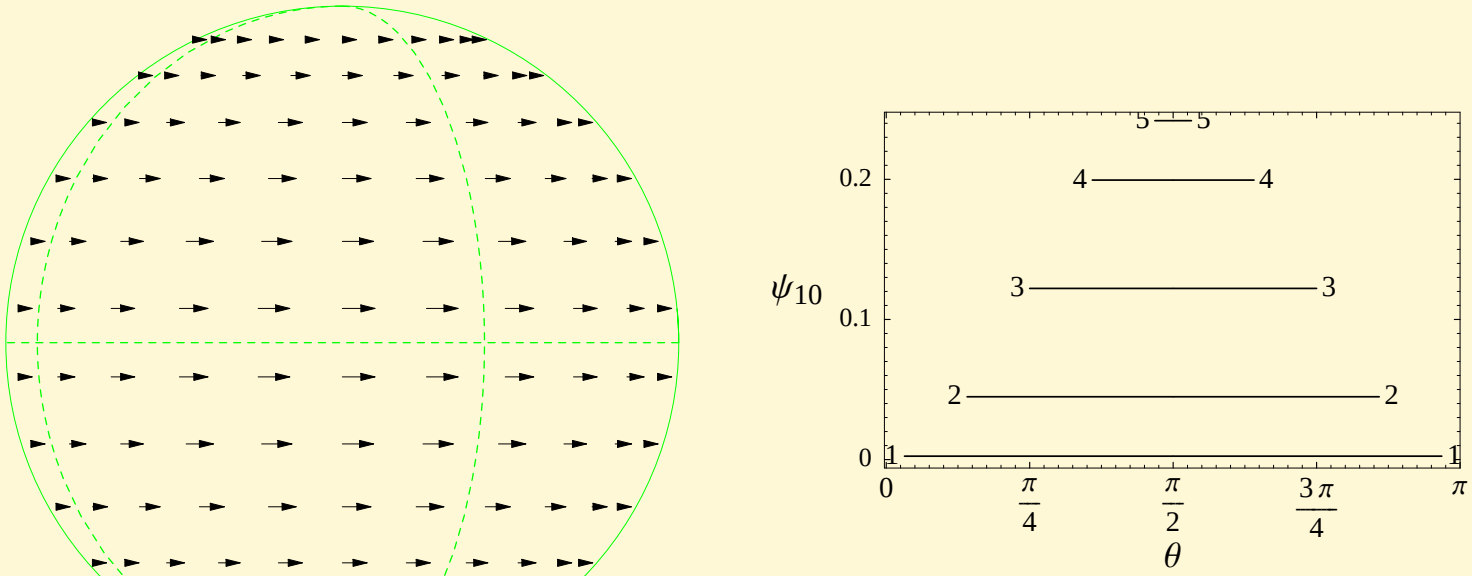

Figure 8: *left*: Velocity field on a sphere for the toroidal mode $(1,0)$ is shown at the time $t = 2\pi n/\omega$, where n is an integer, as projection on the meridional plane $\phi = -115°$. *right*: The potential Ψ^{10}_{GJ} along a dipolar magnetic field line as a function of the polar angle θ is shown for 5 field lines for $t = 2\pi n/\omega$. NB: aligned rotator

Toroidal mode (1,0): GJ charge density

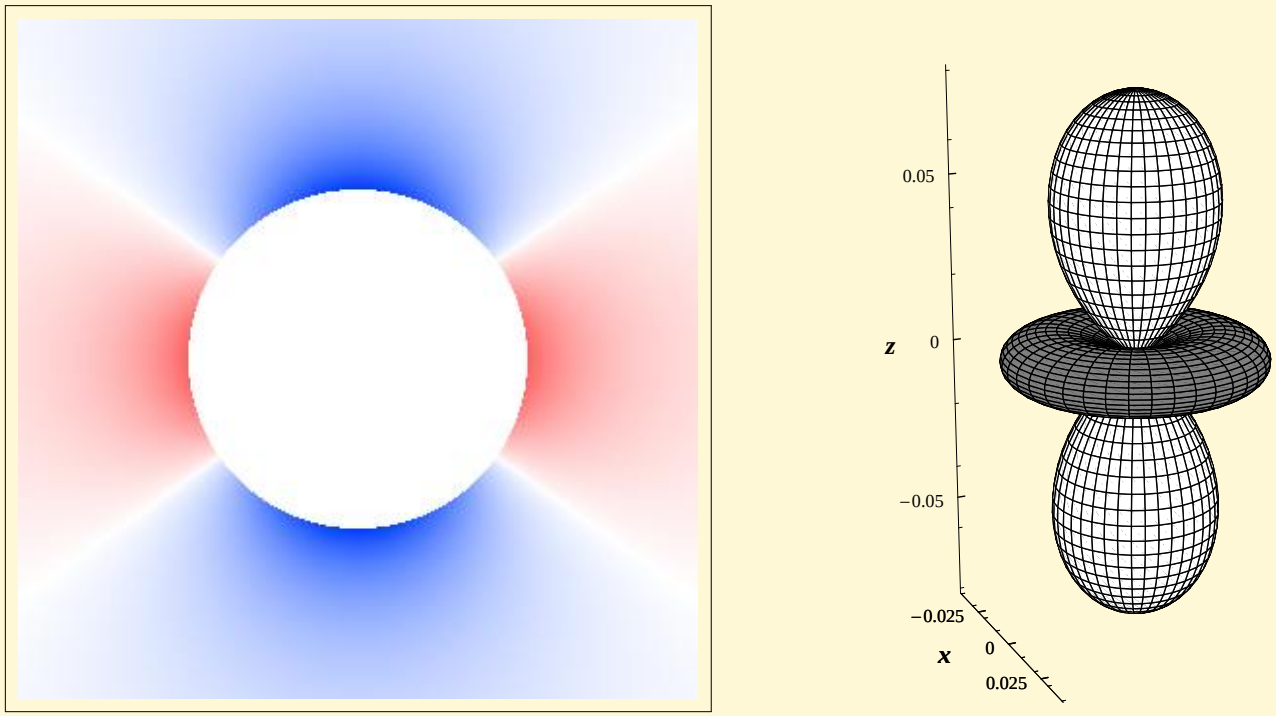

Figure 9: *left*: The charge density ρ_{GJ}^{10} near the NS at $t = 2\pi n/\omega$. Positive values of charge density are shown by red and negative ones by blue color. *right*: The charge density $\rho_{GJ}^{10}|_{r=r_*}$ on the NS surface is shown in a spherical coordinate system $(|\rho_{GJ}^{lm}|_{r=r_*}|, \theta, \phi)$. Positive values of charge density are shown by a gray surface and negative ones by white. NB: aligned rotator

Toroidal mode (2,0)

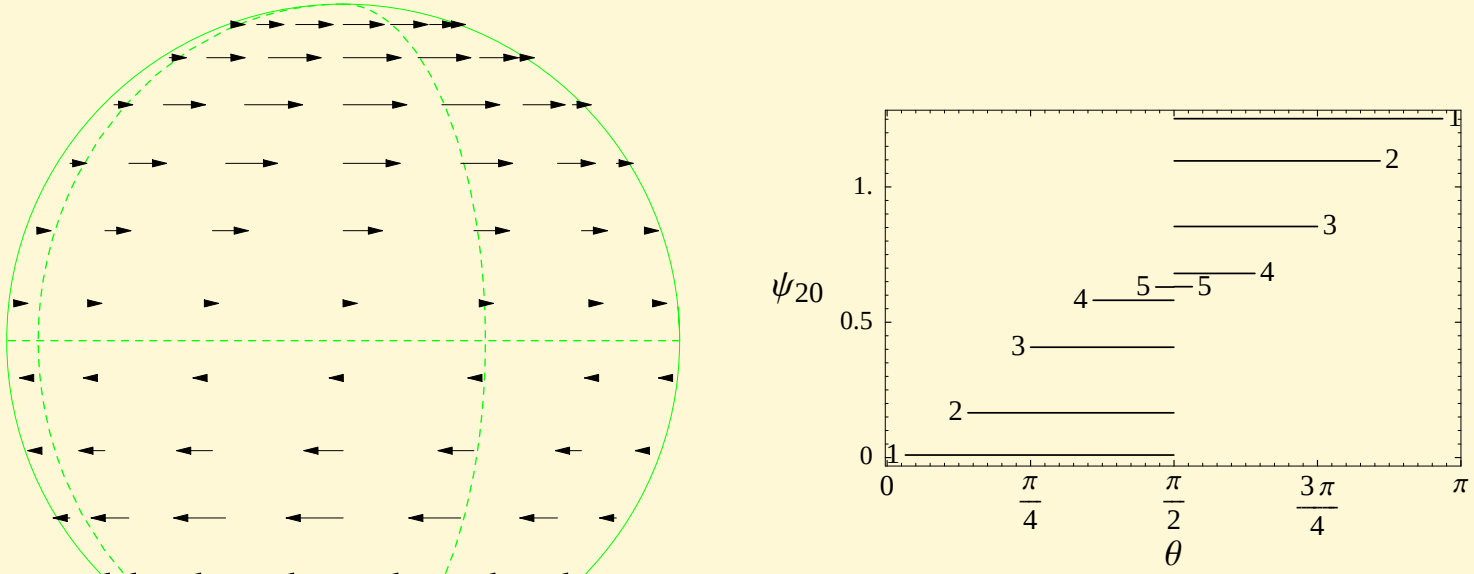

Figure 10: *left*: Velocity fi eld on a sphere for the toroidal mode $(2,0)$ is shown at the time $t = 2\pi n/\omega$, where n is an integer, as projection on the meridional plane $\phi = -115°$. *right*: The potential Ψ^{20}_{GJ} along a dipolar magnetic fi eld line as a function of the polar angle θ is shown for 5 fi eld lines at $t = 2\pi n/\omega$.

Toroidal mode (2,0): GJ charge density

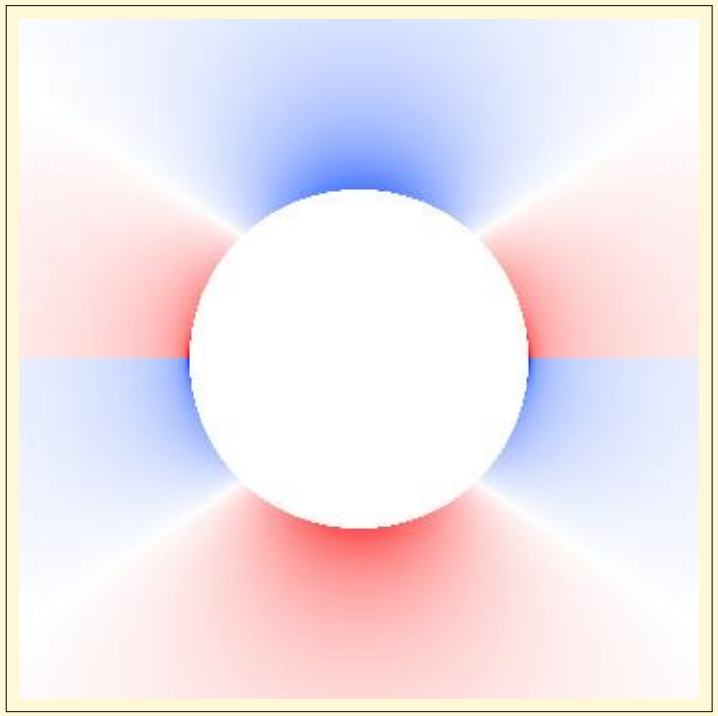

Figure 11: *left*: The charge density ρ_{GJ}^{20} near the NS at $t = 2\pi n/\omega$. Positive values of charge density are shown by red and negative ones by blue color. *right*: The charge density $\rho_{GJ}^{20}|_{r=r_*}$ on the NS surface is shown in a spherical coordinate system $(\left|\rho_{GJ}^{lm}|_{r=r_*}\right|, \theta, \phi)$. Positive values of charge density are shown by the gray surface and negative ones by the white. **NB: on the equatorial plane ($\theta = \pi/2$) ρ_{GJ}^{20} is infinite** .

Toroidal mode (2,1)

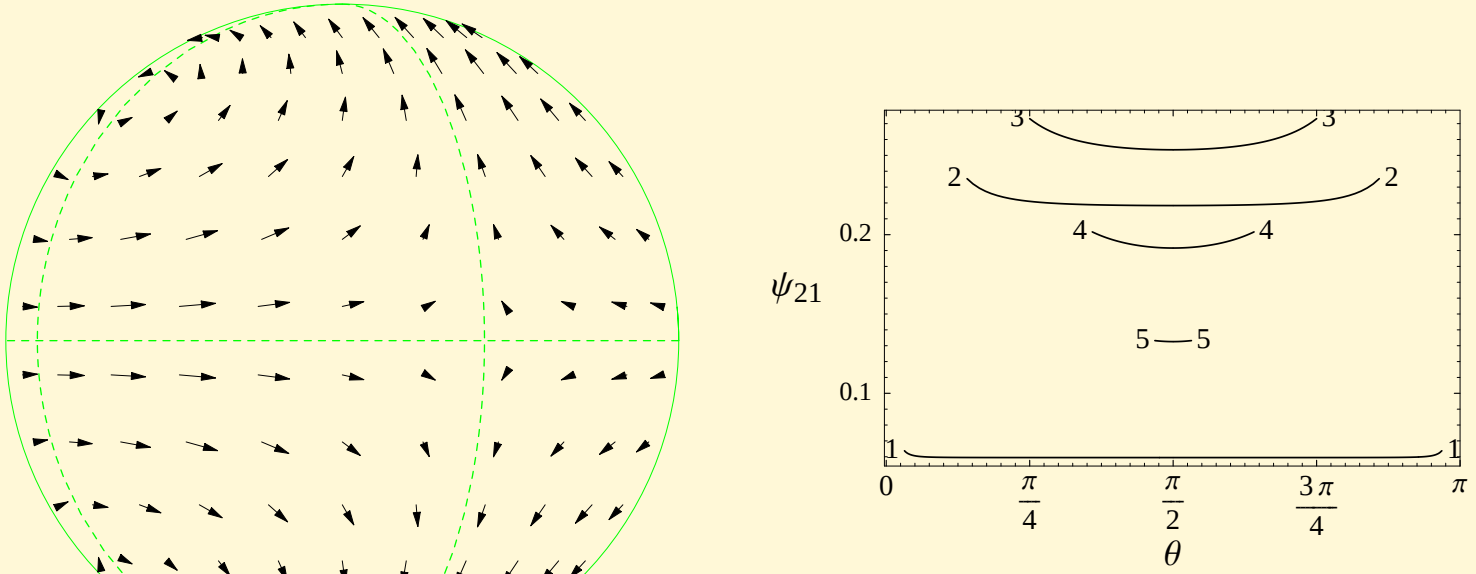

Figure 12: *left*: Velocity fi eld on a sphere for the toroidal mode $(2,1)$ is shown at the time $t = 2\pi n/\omega$, where n is an integer, as projection on the meridional plane $\phi = -115°$. *right*: The potential Ψ_{GJ}^{21} along a dipolar magnetic fi eld line as a function of the polar angle θ is shown for 5 fi eld lines with azimuthal angle $\phi = \pi/2$ at $t = 2\pi n/\omega$.

Toroidal mode (2,1): GJ charge density

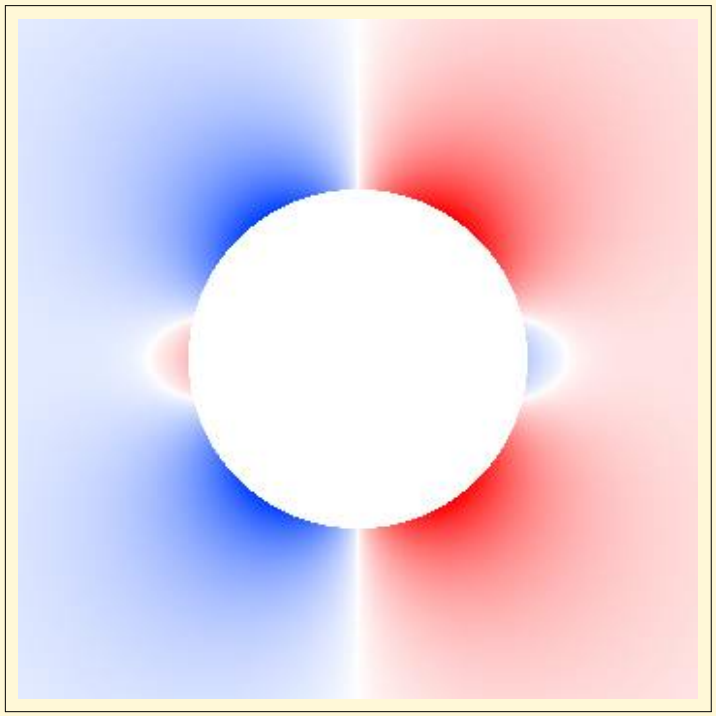

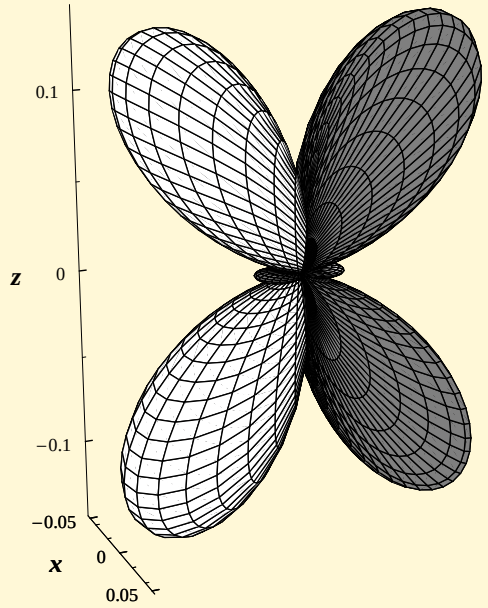

Figure 13: *left*: The charge density ρ_{GJ}^{21} near the NS for azimuthal angle $\phi = \pi/2$ at $t = 2\pi n/\omega$. Positive values of charge density are shown by red and negative ones by blue color. *right*: The charge density $\rho_{GJ}^{21}|_{r=r_*}$ on the NS surface is shown in a spherical coordinate system $(|\rho_{GJ}^{lm}|_{r=r_*}|, \theta, \phi)$. Positive values of charge density are shown by a gray surface and negative ones by white.

Strong current in the magnetosphere

- For toroidal modes with even $(l-m)$, and spheroidal modes with odd $(l-m)$ the strong current with the current density

$$\rho_{GJ}(r_*)\, c\, \left(\frac{c}{\omega r}\right)$$

  should flow along closed magnetic field lines.
- For the open magnetic field lines we could use our solution

Strong current in the magnetosphere

- For toroidal modes with even $(l-m)$, and spheroidal modes with odd $(l-m)$ the strong current with the current density

$$\rho_{GJ}(r_*)\, c\, \left(\frac{c}{\omega r}\right)$$

  should flow along closed magnetic field lines.
- For the open magnetic field lines we could use our solution

Observational manifestations

- This current could generate plasma instabilities and make closed field line regions visible.
- Oscillation modes generating strong current will be more effectively damped.

Glitching Pulsars

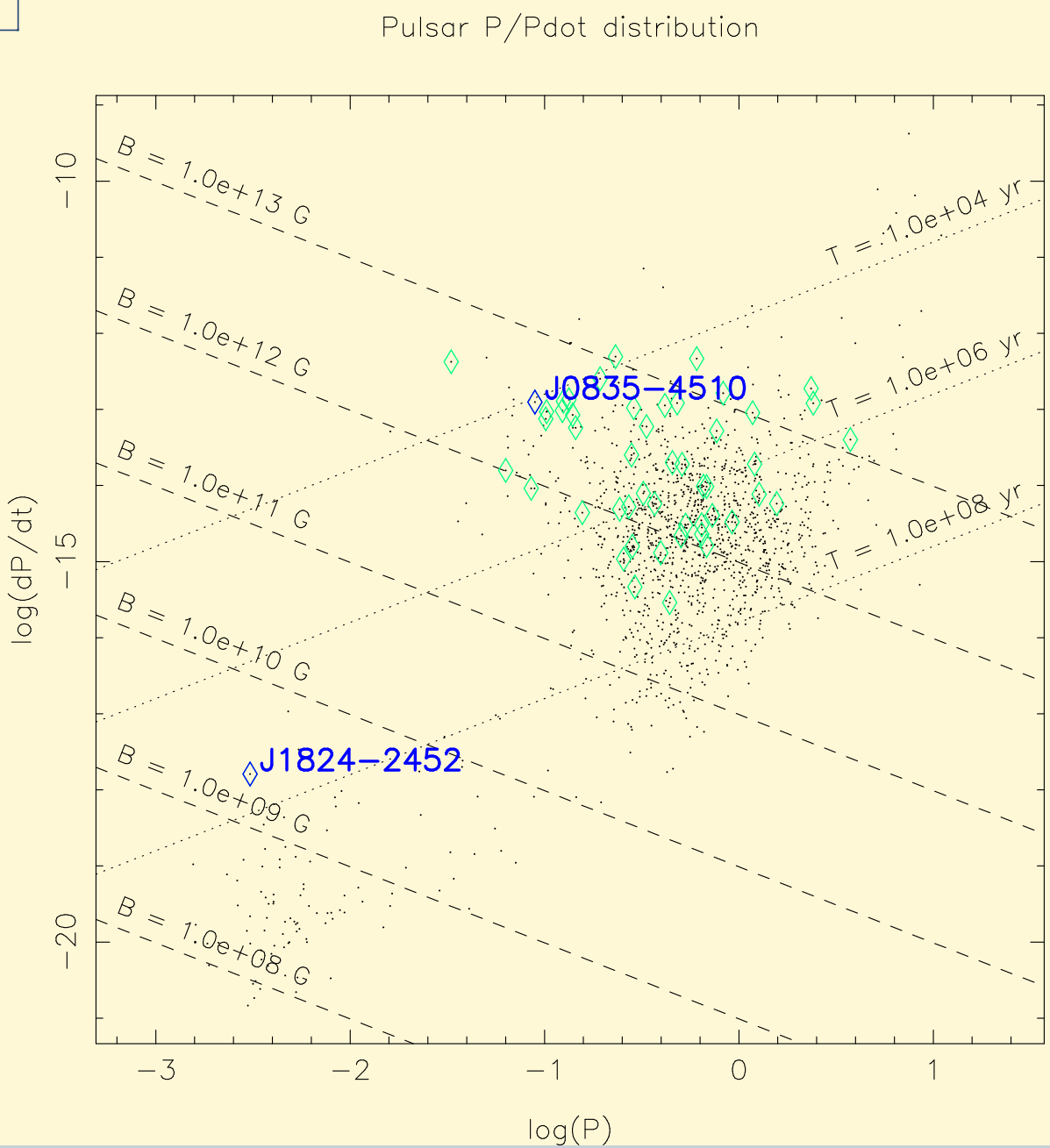

Pulsar $P - \dot{P}$ dot diagram. Pulsars for which one or more glitches have been detected are marked.